This paper describes objective technical results and analysis. Any subjective views or opinions that might be expressed in the paper do not necessarily represent the views of the U.S. Department of Energy or the United States Government.

SAND2018-7689C

Stability Criteria for Power Systems with Damping Control and Asymmetric Feedback Delays

Felipe Wilches-Bernal, *Member, IEEE,* David A. Copp, *Member, IEEE,*
Ian Gravagne, *Senior Member, IEEE,* and David A. Schoenwald, *Senior Member, IEEE,*

***Abstract*—Power system inter-area oscillations can be damped using distributed control of multiple power injections within the interconnection. This type of control traditionally requires system-wide measurements which are transmitted from dispersed, sometimes remote, locations and are subject to delays. This paper evaluates the effect that delayed feedback signals have on the stability of a two-area power system and presents delay-dependent criteria for stability using two different implementations of a damping controller. The controllers are based on a uniform proportional control action and use two feedback signals one from each area of the two-area power system. Each of these signals is subject to an independent delay. Using a Lyapunov-based approach, sufficient conditions for stability that depend on each time delay are found for a range of proportional control gains. Numerical results show that the regions of time delays for which the system is stable are reduced as the proportional gain increases. Time domain simulations validate these stability regions and show the varying responses for the two control implementations and different values of the proportional gain.**

I. Introduction

Small-signal stability analysis in power systems evaluates the capacity of a system to successfully recover and maintain synchronism after a small disturbance. Even though power systems are intricate interconnections of nonlinear components, small-signal stability can be determined by analyzing a linearized version of the system. A particularly important subject within small-signal stability is the study of inter-area oscillations. Also known as global small-signal stability, these oscillations arise when large groups of generators within an area oscillate against those in a different area [1]. Inter-area oscillations appear in power systems spread across large swaths of land and with a sparse concentration of load and generation.

Damping inter-area oscillations is critical to maintain a secure and reliable power grid, and failure to properly address this issue has led to catastrophic consequences. An example is the 1996 blackout throughout the west coast of North America [2]. Power system stabilizers (PSSs), utilizing local measurements, are traditionally used to mitigate this problem. It has also been shown that the use of remote signals in PSSs is advantageous to damping these oscillations [3]. Damping control with system-wide information using distributed resources, system components such as TCSCs, energy storage, and renewable resources has been proposed [4]–[7]. The use of High Voltage DC (HVDC) links in the system for the purpose of damping control has also been proposed and implemented [8], [9]. These works show that damping control of inter-area oscillations benefit from system-wide information. However, remote signals are subject to communication latencies that may impact their applicability in wide-area control.

This paper investigates the impact that delays in feedback signals have on the stability of two different implementations of a wide-area damping controller installed on a power system affected by poorly damped power swings. The two controllers are an HVDC-based controller and an Energy Storage (ES) based controller. Each controller is distributed and uses wide-area measurements from, and acts in, two different locations. Without considering delays, the two controllers are identical and provide sufficient damping of the inter-area oscillations. The presence of delays makes the implementation of the controllers different in practice and affects their transient performance. In previous work, we analyzed time-domain simulations to determine regions of stability of the closed-loop systems that depend on the size of the asymmetric time delays and the control gain [10]. In this work, we derive sufficient conditions for stability of the closed-loop systems modeled as systems of linear delay differential equations (DDEs).

Several techniques for determining sufficient conditions for stability of DDEs with multiple asymmetric time delays exist [11]. Some time domain approaches involve Lyapunov-based stability and utilize a Lyapunov-Razumikhin function [12] or a Lypaunov-Krasovskii function [11], [13], [14]. In this paper, we apply the Lyapunov-Krasovskii stability approach, that was introduced in [11], [13], to determine sufficient conditions for stability of a power system with damping control and multiple asymmetric time delays. Specifically, we find delay-dependent conditions for asymptotic stability of a system of DDEs describing the closed-loop system. These conditions are represented by a system of Linear Matrix Inequalities (LMIs). In addition, we investigate the effect that changing the amount of damping in the system, along with various time delays, has on system stability.

F. Wilches-Bernal, D. Schoenwald, and D. Copp are with Sandia National Laboratories, Albuquerque, NM (e-mail: fwilche@sandia.gov). Ian Gravagne is with the Electrical & Computer Engineering Department at Baylor University, Waco, TX. Sandia National Laboratories is a multimission laboratory managed and operated by National Technology and Engineering Solutions of Sandia, LLC., a wholly owned subsidiary of Honeywell International, Inc., for the U.S. Department of Energy's National Nuclear Security Administration under contract DE-NA0003525.

The authors would like to acknowledge the support of: the BPA Technology Innovation Program, project number TIP 289, Dr. Dmitry Kosterev, POC, with matching funds provided by the U.S. Department of Energy Office of Electricity (DOE/OE) Transmission Reliability Program, Mr. Phil Overholt, and the DOE/OE Energy Storage Program, Dr. Imre Gyuk.

978-1-5386-7138-2/18/$31.00 © 2018 IEEE

II. Power System Dynamics and Damping Control

Power systems are a wide and complex interconnection of multiple components. Due to the nature of these components, and of the power network, the dynamics of interest for small-signal stability can be initially analyzed by simplifying the system, representing each synchronous generator with an electromechanical model (with only two states) and aggregating multiple generators into a single equivalent one intended to represent an entire area. Techniques for generator aggregation and model reduction of power systems are usually based on power system coherency [15]–[17]. In this work, the system of study is shown in Fig. 1 and represents a two-area system with an inter-area oscillation mode.

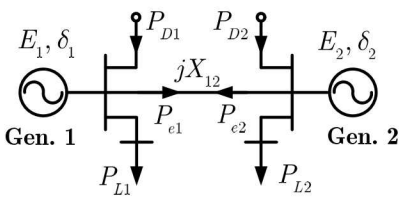

Fig. 1: A two-area power system where each individual area is represented by an aggregated generator.

Representing synchronous generators using the electromechanical model, the dynamics that govern the system in Fig. 1 are [15], [16], for $i = 1, 2$,

$$\dot{\delta}_i = \Omega\omega_i$$
$$2H_i\dot{\omega}_i = P_{mi} - P_{ei} - D_i\omega_i - \frac{1}{R_i}\omega_i - P_{Li} + P_{Di},$$

where the power flow in between the areas is

$$P_{e1} = C_{12}\sin(\delta_1 - \delta_2)$$
$$P_{e2} = C_{21}\sin(\delta_2 - \delta_1)$$

with $C_{12} = Y_{12}E_1E_2$, $C_{21} = Y_{12}E_2E_1$ and $Y_{12} = X_{12}^{-1}$. E_1 and E_2 are the internal voltage angle of the generators, X_{12} is the impedance of the transmission line linking the two areas (which is assumed it is only reactive), and Ω is the per-unit constant used for unit conversion. The power quantities P_{Li}, P_{Di} stand for the aggregated load and a controllable power injection in the ith area, respectively. P_{mi} represents the mechanical power input to the ith machine, and D_i its respective damping. The variables R_i represent the governing droop constant of the area. To study small signal stability, a linear representation of system (1) is obtained. A block diagram of the linear system is shown in Fig. 2, where

$$G_i(s) = \frac{1}{2H_i s + D_i},$$

and H_i is the inertia constant of the machine.

In matrix form, the equations that determine the dynamics of the linearized version of the system are,

$$\begin{bmatrix}\Delta\dot{\delta}(t)\\ \Delta\dot{\omega}(t)\end{bmatrix} = \begin{bmatrix}\mathbf{0} & \Omega I\\ -(2H)^{-1}T_s & -(2H)^{-1}(D+R^{-1})\end{bmatrix}\begin{bmatrix}\Delta\delta(t)\\ \Delta\omega(t)\end{bmatrix}, \tag{2}$$

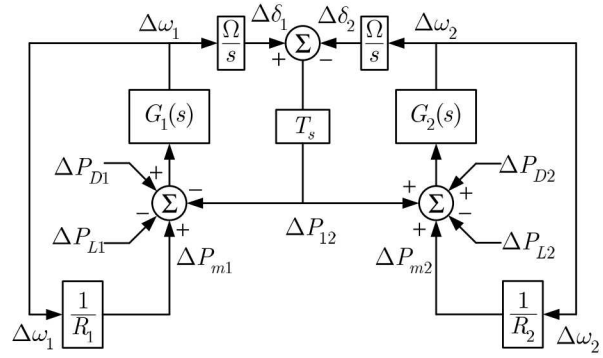

Fig. 2: Block diagram of the linear model of a two-area power system (adapted from [1]).

where $\mathbf{0}$ denotes a matrix of appropriate dimensions with all elements equal to zero, and I denotes the identity matrix. The states of the system are the generators' rotor angles $\Delta\delta(t) = [\Delta\delta_1(t) \;\; \Delta\delta_2(t)]^\top$ and angular velocities $\Delta\omega(t) = [\Delta\omega_1(t) \;\; \Delta\omega_2(t)]^\top$. The matrix in (2) corresponds to the system A matrix. The individual components of A are

$$T_s = \begin{bmatrix}-C_{12}\cos(\bar{\delta}_1 - \bar{\delta}_2) & C_{12}\cos(\bar{\delta}_1 - \bar{\delta}_2)\\ C_{21}\cos(\bar{\delta}_2 - \bar{\delta}_1) & -C_{21}\cos(\bar{\delta}_2 - \bar{\delta}_1)\end{bmatrix},$$

which is the synchronizing torque matrix that has a Laplacian structure. Note that $\bar{\delta}_1$, $\bar{\delta}_2$ is the operating condition (at which the system was linearized) of the rotor angle of Area 1 and 2 respectively. The matrices D, R, and H are defined as

$$D = \begin{bmatrix}D_1 & 0\\ 0 & D_2\end{bmatrix}, \quad R = \begin{bmatrix}R_1 & 0\\ 0 & R_2\end{bmatrix}, \quad H = \begin{bmatrix}H_1 & 0\\ 0 & H_2\end{bmatrix}.$$

The system (2) has four eigenvalues. Due to the Laplacian nature of T_s, one of the eigenvalues is at the origin, and it is known as the system mode. Because the damping and droop coefficients D_i and R_i, respectively, are positive, the remaining three eigenvalues lie in the left-half plane. The input matrices for variations on the power injections $P_D = [P_{D1} \;\; P_{D2}]^\top$ and aggregated loads $P_L = [P_{L1} \;\; P_{L2}]^\top$ are

$$B_D = \begin{bmatrix}\mathbf{0}\\ (2H)^{-1}\end{bmatrix}, \qquad B_L = \begin{bmatrix}\mathbf{0}\\ -(2H)^{-1}\end{bmatrix}.$$

Therefore, defining the state as $x(t) = [\Delta\delta(t)^\top \;\; \Delta\omega(t)^\top]^\top$, the linear dynamics for the two-area power system in Fig. 2 can be written as

$$\dot{x}(t) = Ax(t) + B_D P_D + B_L P_L. \tag{3}$$

A. Damping Control

Because the system in Fig. 2 is intended to represent a power system prone to inter-area oscillations, it traditionally has a pair of eigenvalues with low damping, which correspond to the inter-area oscillation of the power system. This type of system can be effectively stabilized by using a controller of the form,

$$P_{D1}(t) = -k_d(\Delta\omega_1(t) - \Delta\omega_2(t)) \tag{4a}$$
$$P_{D2}(t) = -P_{D1}(t) = k_d(\Delta\omega_1(t) - \Delta\omega_2(t)), \tag{4b}$$

where k_d is a gain that can be chosen. The power injections into each area of the system, P_{D1} and P_{D2}, act with equal magnitude but opposite sign. This type of control action for the wNAPS has been proposed and successfully implemented [8]. The controller equations (4) can be rewritten as

$$K(t) = \begin{bmatrix} \mathbf{0} & K_c \end{bmatrix} x(t),$$

where K_c is a gain matrix given by

$$K_c = \begin{bmatrix} -k_d & k_d \\ k_d & -k_d \end{bmatrix}.$$

Because control is performed by modulating the power injections P_{Di}, the multiplication of $K(t)$ with B_D determines the additional dynamics the controller imposes on the system. Therefore, the system (3) can be rewritten as

$$\begin{aligned} \dot{x}(t) &= Ax(t) + B_D K(t) + B_L P_L \\ &= A_{cl} x(t) + B_L P_L, \end{aligned}$$

where

$$A_{cl} = \begin{bmatrix} \mathbf{0} & \Omega I \\ -(2H)^{-1} T_s & -(2H)^{-1}(D + R^{-1} - K_c) \end{bmatrix}.$$

B. Delay in the Feedback Signals

Power systems with dominant inter-area oscillations tend to be dispersed and usually encompass large geographical areas. In such types of systems, the implementation of the controller (4) involves the transfer of information from distant regions and is, therefore, subject to delays. This section presents the effect that different time delays have in two different implementations of this controller. Note that these types of controllers are known as wide-area controllers and are possible in power systems due to the deployment of Phasor Measurement Unit (PMU) technology [18].

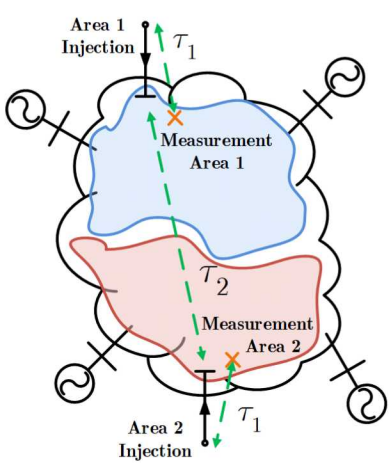

Fig. 3: Power injections and measurements delay in a two-area power system.

1) Damping Control using HVDC: The controller in (4) can be implemented using a controllable HVDC transmission line. In this scenario there is only one controller with two different actuation points, and the equations (4a)-(4b) with the inclusion of time delays, τ_1 and τ_2, (neglecting losses) become

$$P_{D1}(t) = -k_d(\Delta\omega_1(t-\tau_1) - \Delta\omega_2(t-\tau_2)) \quad (5a)$$
$$P_{D2}(t) = k_d(\Delta\omega_1(t-\tau_1) - \Delta\omega_2(t-\tau_2)). \quad (5b)$$

With this implementation, $P_{D1}(t) = -P_{D2}(t)$ due to the symmetric nature of an HVDC system. The dynamics of the closed loop system (neglecting the aggregated loads P_L) can be expressed by the following DDE

$$\dot{x}(t) = Ax(t) + A_1^{\text{HV}} x(t-\tau_1) + A_2^{\text{HV}} x(t-\tau_2), \quad (6)$$

where

$$A_1^{\text{HV}} = \begin{bmatrix} 0 & 0 & 0 & 0 \\ 0 & 0 & 0 & 0 \\ 0 & 0 & \frac{-k_d}{2H_1} & 0 \\ 0 & 0 & \frac{k_d}{2H_2} & 0 \end{bmatrix}, \; A_2^{\text{HV}} = \begin{bmatrix} 0 & 0 & 0 & 0 \\ 0 & 0 & 0 & 0 \\ 0 & 0 & 0 & \frac{k_d}{2H_1} \\ 0 & 0 & 0 & \frac{-k_d}{2H_2} \end{bmatrix}.$$

Fig. 3 shows a diagram of the damping controller. In the case of HVDC implementation, the single controller located in either area is subject to two communication delays. If the controller is located in Area 1, the measurement from Area 1 is the local one and will be subject to a delay of τ_1. The remote measurement from Area 2 is subject to τ_2.

2) Damping Control using Energy Storage: Similarly, the controller in (4) can be implemented using a pair of complementary Energy Storage (ES) devices with one located in each area. In such a case, each controller is subject to its own set of delays as depicted in Fig. 3. The controller located in Area 1 is subject to the same delays as in the HVDC case, where the remote measurement from Area 2 (remote for the controller in Area 1) is subject to τ_2, and the measurement from Area 1 is subject to τ_1 (local measurement for the Area 1 controller). However, the controller in Area 2 observes a different set of delays: The measurement from Area 1 is now subject to τ_2 (because, for the controller in Area 2, the measurement in Area 1 is remote), while the Area 2 measurement is subject to τ_1. Hence, the equations describing the controller (4), using ES components, in the presence of delays become

$$P_{D1}(t) = -k_d(\Delta\omega_1(t-\tau_1) - \Delta\omega_2(t-\tau_2)) \quad (7a)$$
$$P_{D2}(t) = k_d(\Delta\omega_1(t-\tau_2) - \Delta\omega_2(t-\tau_1)). \quad (7b)$$

The closed loop dynamics of the system with damping control using ES (again neglecting aggregated loads P_L) can then be expressed with the following DDE

$$\dot{x}(t) = Ax(t) + A_1^{\text{ES}} x(t-\tau_1) + A_2^{\text{ES}} x(t-\tau_2), \quad (8)$$

where

$$A_1^{\text{ES}} = \begin{bmatrix} 0 & 0 & 0 & 0 \\ 0 & 0 & 0 & 0 \\ 0 & 0 & \frac{-k_d}{2H_1} & 0 \\ 0 & 0 & 0 & \frac{-k_d}{2H_1} \end{bmatrix} \; A_2^{\text{ES}} = \begin{bmatrix} 0 & 0 & 0 & 0 \\ 0 & 0 & 0 & 0 \\ 0 & 0 & 0 & \frac{k_d}{2H_1} \\ 0 & 0 & \frac{k_d}{2H_1} & 0 \end{bmatrix}$$

Note that only differences in the DDEs describing the closed loop dynamics (6) and (8) are the matrices A_1^{ES}, A_1^{HV} and A_2^{ES}, A_2^{HV}.

Because the systems in (6) and (8) have a Laplacian matrix T_s within their structure, they retain the eigenvalue at $(0,0)$, which is unaffected by both the delays and the proportional gain k_d. To be able to analyze the stability of the system, the size of the system is reduced by combining the two rotor angle states $\delta_1(t)$ and $\delta_2(t)$ into a single one: $\delta_{12}(t) = \delta_1(t) - \delta_2(t)$. This state transformation reduces equations (6) and (8) to third order. These reduced state equations are used in this paper henceforth.

Even though it is natural to assume that local information delay is smaller than remote delay, for full generality, in this work no assumptions are made about the size of the delays. In practice, these delays depend on the communication channels linking the controller and the remote measurement devices.

III. Stability Criteria for Systems with Two Asymmetric Time Delays

In this section we present a Lyapunov-Krasovskii approach to determining delay-dependent stability criteria for the systems (6) and (8). The following theorem, first introduced in [13], gives delay-dependent criteria for asymptotic stability of DDEs of the same form as (6) and (8). Further discussion of this result, including discussion of its conservativeness as compared to other related results, can be found in [11], [13].

For this result, we generically write systems (6) and (8) as

$$\dot{x}(t) = Ax(t) + A_1 x(t-\tau_1) + A_2 x(t-\tau_2). \tag{9}$$

Theorem 1 (Asymptotic stability [13, Theorem 1])**.** *The system* (9)*, with time delays $\tau_i \geq 0$, $i = 1,2$, is asymptotically stable if there exist symmetric positive definite matrices $P = P^\top > 0$ and $Q_i = Q_i^\top > 0$, $i = 1,2$, symmetric positive semi-definite matrices $W_i = W_i^\top \geq 0$, $X_{ii} =^\top \geq 0$, $Y_{ii} = Y_{ii}^\top \geq 0$, $Z_{ii} = Z_{ii}^\top \geq 0$, $i = 1,2,3$, and any matrices N_i, S_i, L_i, $i = 1,2,3$, and X_{ij}, Y_{ij}, Z_{ij}, $1 \leq i < j \leq 3$, such that the following LMIs hold*

$$\Phi = \begin{bmatrix} \Phi_{11} & \Phi_{12} & \Phi_{13} \\ \Phi_{12}^\top & \Phi_{22} & \Phi_{23} \\ \Phi_{13}^\top & \Phi_{23}^\top & \Phi_{33} \end{bmatrix} < 0, \tag{10a}$$

$$\Psi_1 = \begin{bmatrix} X_{11} & X_{12} & X_{13} & N_1 \\ X_{12}^\top & X_{22} & X_{23} & N_2 \\ X_{13}^\top & X_{23}^\top & X_{33} & N_3 \\ N_1^\top & N_2^\top & N_3^\top & W_1, \end{bmatrix} \geq 0, \tag{10b}$$

$$\Psi_2 = \begin{bmatrix} Y_{11} & Y_{12} & Y_{13} & S_1 \\ Y_{12}^\top & Y_{22} & Y_{23} & S_2 \\ Y_{13}^\top & Y_{23}^\top & Y_{33} & S_3 \\ S_1^\top & S_2^\top & S_3^\top & W_2, \end{bmatrix} \geq 0, \tag{10c}$$

$$\Psi_3 = \begin{bmatrix} Z_{11} & Z_{12} & Z_{13} & kL_1 \\ Z_{12}^\top & Z_{22} & Z_{23} & kL_2 \\ Z_{13}^\top & Z_{23}^\top & Z_{33} & kL_3 \\ kL_1^\top & kL_2^\top & kL_3^\top & W_3, \end{bmatrix} \geq 0, \tag{10d}$$

where

$$k = \begin{cases} 1 & \text{if} \quad \tau_1 \geq \tau_2, \\ -1 & \text{if} \quad \tau_1 < \tau_2. \end{cases}$$

The elements of Φ are defined as

$$\begin{aligned}
\Phi_{11} =& PA + A^\top P + Q_1 + Q_2 + N_1 + N_1^\top + S_1 + S_1^\top \\
&+ A^\top TA + \tau_1 X_{11} + \tau_2 Y_{11} + k(\tau_1 - \tau_2) Z_{11}, \\
\Phi_{12} =& PA_1 - N_1 + N_2^\top + S_2^\top - L_1 + A^\top TA_1 \\
&+ \tau_1 X_{12} + \tau_2 Y_{12} + k(\tau_1 - \tau_2) Z_{12}, \\
\Phi_{13} =& PA_2 + N_3^\top + S_3^\top - S_1 + L_1 + A^\top TA_2 \\
&+ \tau_1 X_{13} + \tau_2 Y_{13} + k(\tau_1 - \tau_2) Z_{13}, \\
\Phi_{22} =& -Q_1 - N_2 - N_2^\top - L_2 - L_2^\top + A_1^\top TA_1 \\
&+ \tau_1 X_{22} + \tau_2 Y_{22} + k(\tau_1 - \tau_2) Z_{22}, \\
\Phi_{23} =& -N_3^\top - S_2 + L_2 - L_3^\top + A_1^\top TA_2 \\
&+ \tau_1 X_{23} + \tau_2 Y_{23} + k(\tau_1 - \tau_2) Z_{23}, \\
\Phi_{33} =& -Q_2 - S_3 - S_3^\top + L_3 + L_3^\top + A_2^\top TA_2 \\
&+ \tau_1 X_{33} + \tau_2 Y_{33} + k(\tau_1 - \tau_2) Z_{33},
\end{aligned}$$

where $T = \tau_1 W_1 + \tau_2 W_2 + k(\tau_1 - \tau_2) W_3$.

Proof. The proof can be found in [11], [13] using the Lyapunov-Krasovskii functional:

$$\begin{aligned}
V(x(t)) = V_1(x(t)) + V_2(x(t)) + V_3(x(t)) \\
+ V_4(x(t)) + V_5(x(t)) + V_6(x(t)),
\end{aligned}$$

where

$$\begin{aligned}
V_1(x(t)) &= x(t)^\top P x(t) \\
V_2(x(t)) &= \int_{t-\tau_1}^{t} x^\top(s) Q_1 x(s) \mathrm{d}s \\
V_3(x(t)) &= \int_{t-\tau_2}^{t} x^\top(s) Q_2 x(s) \mathrm{d}s \\
V_4(x(t)) &= \int_{-\tau_1}^{0} \int_{t+\theta}^{t} \dot{x}^\top(s) W_1 \dot{x}(s) \mathrm{d}s \mathrm{d}\theta \\
V_5(x(t)) &= \int_{-\tau_2}^{0} \int_{t+\theta}^{t} \dot{x}^\top(s) W_2 \dot{x}(s) \mathrm{d}s \mathrm{d}\theta \\
V_6(x(t)) &= \int_{-\tau_1}^{-\tau_2} \int_{t+\theta}^{t} \dot{x}^\top(s) W_3 \dot{x}(s) \mathrm{d}s \mathrm{d}\theta,
\end{aligned}$$

and $\theta \in [-\tau_1, 0]$.

□

In the next section, we present numerical results showing the regions of asymptotic stability determined from the criteria in Theorem 1 for examples of systems (6) and (8).

IV. Numerical Results

The test system of this study is the two-area power system shown in Fig. 2. It is assumed that the two areas are identical with the parameters given as, $D_1 + {}^1/_{R_1} = D_2 + {}^1/_{R_2} = 0.1$, $H_1 = H_2 = 5/2$, and $T_s = 14$. With these parameter values, the open-loop system (when $k_d = 0$) has a complex pair of eigenvalues located at $-0.01 \pm 2.336j$, which corresponds to the least damped inter-area mode of the system. This mode of oscillation is damped by increasing k_d as is shown in Fig. 4. These results show that when no delay is considered, the modes of the inter-area oscillation move further to the left

in the left-half plane, thereby improving the overall stability of the system. In this section, the effects of including delay in the feedback signals on the stability of the system are presented. The results are derived from Theorem 1. Several values for the controller gain k_d and time delays τ_1 and τ_2 are considered. In addition, several time-domain simulations are presented and analyzed in order to validate the regions of stability determined from Theorem 1.

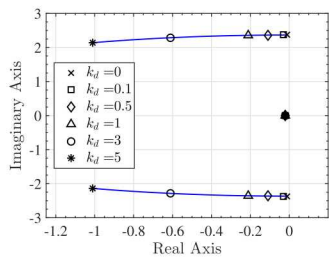

Fig. 4: Effect of increasing k_d on the modes of the system in closed loop (without considering delays). Note that the eigenvalue at -0.02 is not affected by variations in k_d.

A. Regions of Stability

The stability regions for the linearized two-area power system (2), as shown in Fig. 2, with the parameters given above can be computed by solving the LMI conditions (10d) in Theorem 1. Because the conditions in Theorem 1 are only sufficient conditions, these results are expected to be conservative. Solving the LMIs (10d) for both systems (6) and (8) results in the same stability regions, and the resulting stability regions are shown in Fig. 5. Note that although the regions in Fig. 5 are sufficient conditions for stability of both system (6) and (8), the two systems exhibit different responses to loads P_L. This can clearly be seen in the first swing of the time domain simulations in Fig. 8 below. Fig. 5 shows that, for all values of k_d shown, the systems (6) and (8) are asymptotically stable if both τ_1 and τ_2 are relatively small or if at least one delay, τ_1 or τ_2, is very close to zero. As the value of the controller gain increases, Fig. 5 shows that the regions of stability shrink. This is counter-intuitive as increasing the controller gain k_d increases damping and causes the poles of the non-delayed system to move further to the left in the left-half plane (as seen in Fig. 4). Therefore, both systems are less robust to time delays as the gain k_d increases. The time domain simulations in the next section verify this.

B. Simulations in Time Domain

The time simulations in this section, presented to validate the validating the regions of stability shown in Fig. 5, show each system's response to a sudden change in load after 1 second, represented as a step function in P_{L1}. Fig. 6 shows time simulation results when the delays considered are $\tau_1 = \tau_2 = 0.4$ and $\tau_1 = \tau_2 = 0.6$. In this case, because the delays are identical, both the HVDC implementation of the controller in (5) and the ES implementation of the controller in (7) are equivalent. The results in Fig. 6 show that for identical delays $\tau_1 = \tau_2 = 0.4$, the systems are always stable and that increasing k_d improves the damping. However, when the delays are increased to $\tau_1 = \tau_2 = 0.6$, both systems are highly unstable for the larger values of the proportional gain ($k_d = 3$ and $k_d = 5$). This means that the values of k_d that provide a strong stabilizing effect when the delays are smaller are highly destabilizing when the delays are larger. Fig. 7 also shows a case where an increase in k_d (in this case from 3 to 5) changes the effect of the controller from effectively providing damping to destabilizing both systems. As mentioned before, the regions of stability shown in Fig 5 may be conservative. Fig. 6b highlights this fact because, even though the point $\tau_1 = \tau_2 = 0.6$ is not in the region shown in Fig. 5c when $k_d = 0.5$, the time simulation shows that the systems (6) and (8) are stable when $k_d = 0.5$ and $\tau_1 = \tau_2 = 0.6$.

Figs. 8a-8b show time simulations, for both controller implementations, when the delays are $\tau_1 = 0$ and $\tau_2 = 1.0$. These results show that increases in gain always provide damping to the system. That is, if only one signal is delayed, even with large delay, as long as the other has no (or very small) time delay, the controller still stabilizes both systems (by providing damping). Figs. 8c-8d show the same results when the delays are reversed and take values of $\tau_1 = 1.0$ and $\tau_2 = 0.0$. These results validate the regions of stability

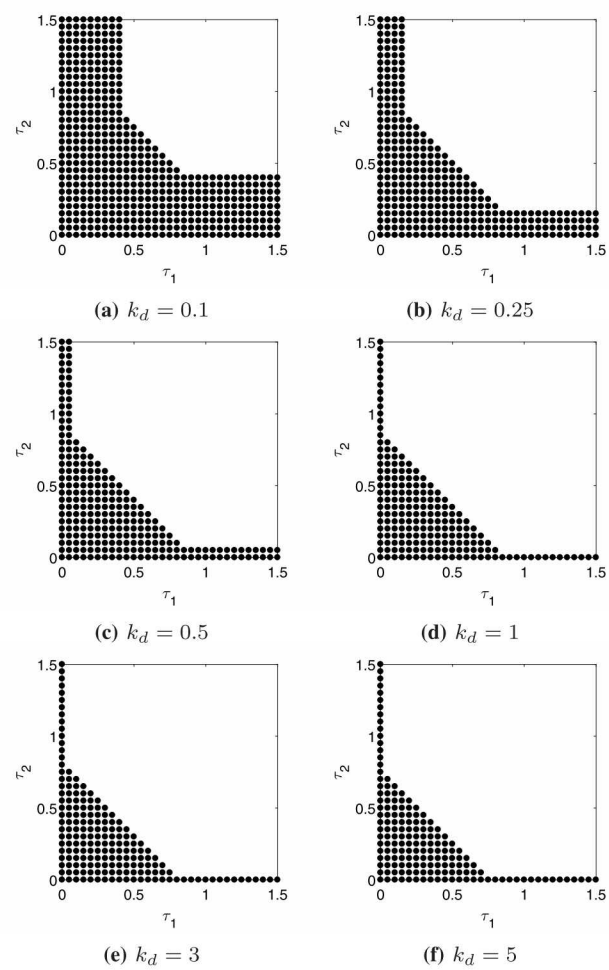

(a) $k_d = 0.1$ **(b)** $k_d = 0.25$ **(c)** $k_d = 0.5$ **(d)** $k_d = 1$ **(e)** $k_d = 3$ **(f)** $k_d = 5$

Fig. 5: Regions of stability for systems (6) and (8) derived from Theorem 1 with the HVDC controllers (5a)-(5b) and ES controllers (7a)-(7b), respectively, with several values for the proportional gain k_d.

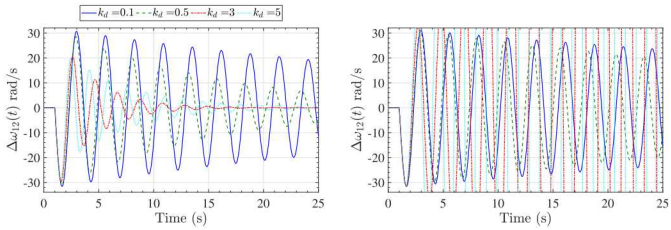

(a) ES and HVDC with $\tau_1 = \tau_2 = 0.4$ **(b)** ES and HVDC with $\tau_1 = \tau_2 = 0.6$

Fig. 6: Time simulations for the test system with different implementations of the controller. The delays considered are symmetric and with values of $\tau_1 = \tau_2 = 0.4$ and $\tau_1 = \tau_2 = 0.6$.

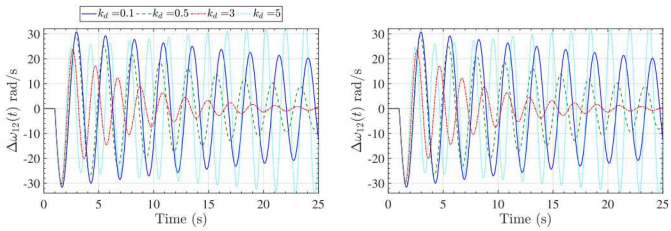

(a) ES with $\tau_1 = 0.4$ and $\tau_2 = 0.5$ **(b)** HVDC with $\tau_1 = 0.4$ and $\tau_2 = 0.5$

Fig. 7: Time simulations for the test system with different implementations of the controller. The delays considered are $\tau_1 = 0.4$ and $\tau_2 = 0.5$.

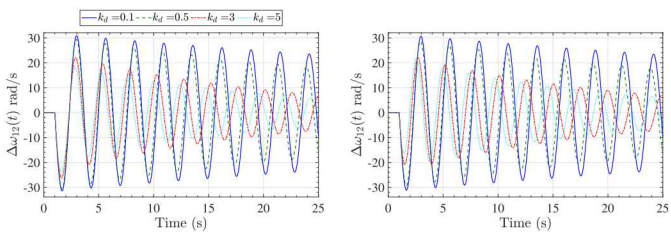

(a) ES with $\tau_1 = 0$ and $\tau_2 = 1.0$ **(b)** HVDC with $\tau_1 = 0$ and $\tau_2 = 1.0$

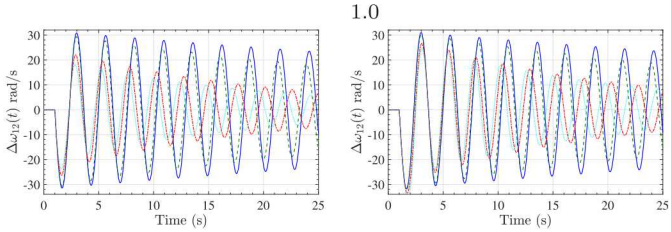

(c) ES with $\tau_1 = 1.0$ and $\tau_2 = 0$ **(d)** HVDC with $\tau_1 = 1.0$ and $\tau_2 = 0$

Fig. 8: Time simulations for the test system with different implementations of the controller. The delays considered are $\tau_1 = 0.0$ and $\tau_2 = 1.0$ in (a) and (b) and $\tau_1 = 1.0$ and $\tau_2 = 0.0$ in (c) and (d).

appearing in Fig. 5 along both the τ_1 and τ_2 axes.

V. Conclusions

This paper studies the effect that multiple asymmetric time delays have on the stability of a two-area power system with a dominant inter-area oscillation. Two different distributed control implementations based on a proportional action that modulates power injections in each area of the system were proposed for damping this oscillation. The controllers' feedback signals, which come from both areas of the system, are subject to asymmetric delays. Using a Lyapunov-Krasovskii approach, the paper presents delay-dependent criteria under which the feedback systems are asymptotically stable. From these criteria, regions of stability are derived for several values of the proportional control gain k_d. Numerical results show that while increasing the proportional control gain is beneficial for damping the oscillation when the delays are small, the effect is inverted for larger delays, causing the systems to go unstable. Therefore, the systems are less robust to larger delays when higher values of k_d are chosen.

References

[1] P. Kundur, *Power System Stability and Control*. New York, NY: McGraw-Hill, 1994.

[2] D. N. Kosterev, C. W. Taylor, and W. Mittelstadt, "Model validation for the August 10, 1996 WSCC system outage," *IEEE Trans. Power Syst.*, vol. 14, no. 3, pp. 967–979, Aug. 1999.

[3] J. H. Chow, J. J. Sanchez-Gasca, H. Ren, and S. Wang, "Power system damping controller design using multiple input signals," *IEEE Control Syst. Mag.*, vol. 20, no. 4, pp. 82–90, Aug. 2000.

[4] A. Chakrabortty, "Wide-area damping control of power systems using dynamic clustering and TCSC-based redesigns," *IEEE Trans. Smart Grid*, vol. 3, no. 3, pp. 1503–1514, Sept. 2012.

[5] F. Dörfler, M. R. Jovanovic, M. Chertkov, and F. Bullo, "Sparsity-promoting optimal wide-area control of power networks," *IEEE Transactions on Power Systems*, vol. 29, no. 5, pp. 2281–2291, Feb. 2014.

[6] J.C. Neely *et al.*, "Damping of inter-area oscillations using energy storage," in *Power and Energy Soc. General Meeting, 2013 IEEE*, Vancouver, BC, 2013, pp. 1–5.

[7] F. Wilches-Bernal, C. Lackner, and J. H. Chow, "Power system controllability through nontraditional generation," in *55th Annu. Conf. on Decision and Control (CDC), 2016 IEEE*, Las Vegas, NV, 2016, pp. 702–708.

[8] D. Trudnowski, B. Pierre, F. Wilches-Bernal, D. Schoenwald, R. Elliott, J. Neely, R. Byrne, and D. Kosterev, "Initial closed-loop testing results for the Pacific DC Intertie wide area damping controller," in *Power and Energy Soc. General Meeting, 2017. IEEE*, Chicago, IL, 2017, pp. 1–5.

[9] D. A. Schoenwald, B. J. Pierre, F. Wilches-Bernal, and D. J. Trudnowski, "Design and implementation of a wide-area damping controller using high voltage dc modulation and synchrophasor feedback," *IFAC-PapersOnLine*, vol. 50, no. 1, pp. 67–72, 2017.

[10] D. A. Copp, F. Wilches-Bernal, I. Gravagne, and D. A. Schoenwald, "Time-domain analysis of power system stability with damping control and asymmetric feedback delays," in *the 2017 North American Power Symposium (NAPS)*, 2017, pp. 1–6.

[11] M. Wu, Y. He, and J.-H. She, *Stability analysis and robust control of time-delay systems*. Springer, 2010.

[12] Z.-J. Tang, T.-Z. Huang, J.-L. Shao, and J.-P. Hu, "Consensus of second-order multi-agent systems with nonuniform time-varying delays," *Neurocomputing*, vol. 97, pp. 410–414, 2012.

[13] Y. He, M. Wu, and J.-H. She, "Delay-dependent stability criteria for linear systems with multiple time delays," *IEE Proceedings-Control Theory and Applications*, vol. 153, no. 4, pp. 447–452, 2006.

[14] F. R. Safaei, S. G. Ghiocel, J. P. Hespanha, and J. H. Chow, "Stability of an adaptive switched controller for power system oscillation damping using remote synchrophasor signals," in *53rd Annu. Conf. on Decision and Control (CDC), 2014 IEEE*, Los Angeles, CA, 2014, pp. 1695–1700.

[15] J. H. Chow, *Time-scale modeling of dynamic networks with applications to power systems*. New York, NY: Springer-Verlag, 1982.

[16] ——, *Power System Coherency and Model Reduction*. New York, NY: Springer, 2013.

[17] D. Romeres, F. Dörfler, and F. Bullo, "Novel results on slow coherency in consensus and power networks," in *2013 European Control Conference (ECC)*, Zurich, Switzerland, 2013, pp. 742–747.

[18] A. Chakrabortty and P. P. Khargonekar, "Introduction to wide-area control of power systems," in *American Control Conference (ACC), 2013*. IEEE, 2013, pp. 6758–6770.